Amorphization of Si using cluster ions

Lucia Romano[a] and Kevin S. Jones
Department of Materials Science and Engineering, University of Florida, Gainesville, Florida 32611

Karuppanan Sekar and Wade A. Krull
SemEquip, Inc., 34 Sullivan Road, North Billerica, Massachusetts 01862

(Received 14 October 2008; accepted 2 February 2009; published 9 March 2009)

Amorphization process associated with cluster implants has been studied by cross-sectional transmission electron microscopy for P_4 cluster implants (5 keV equivalent monomer energy) as a function of dose and compared to that of monomer P implant at the same equivalent energy. Amorphous pockets are formed by the cluster implant at doses of as low as $6\times10^{13}/\mathrm{cm}^2$, and a continuous amorphous layer is formed at dose of $2\times10^{14}/\mathrm{cm}^2$. The reduction by about 2.5 times in amorphization threshold by clusters with respect to the monomer implant is a consequence of the simultaneous deposition of energy carried by the atoms in the clusters, which enhances the damage yield in the overlapped collision cascades. © *2009 American Vacuum Society.*
[DOI: 10.1116/1.3089372]

I. INTRODUCTION

Cluster ion beams[1] have attracted significant interest for the possibility of increased dose rate, self-amorphizing, and lower implant energy required to match the stringent needs of ultrashallow junction fabrication. Amorphization is a critical step in the process as the subsequent solid phase epitaxial regrowth can lead to improved dopant activation upon annealing.[2,3] For this reason, it is of fundamental importance to fully characterize the damage amount and morphology produced by cluster ion beam.

Ion beam induced amorphization of Si is the result of a complex balance between the damage generation and its recovery. When ions strike crystalline silicon, they create zones of disorder that exhibit several configurations, ranging from isolated defects or amorphous pockets to continuous amorphous layer. In spite of intense experimental and modeling work,[4] a complete understanding of this critical process in terms of dependence on ion mass, energy, dose, substrate temperature, and dose rate is still lacking. At a fixed temperature, the depth of amorphous-crystalline interface and the amount of residual damage beyond it strongly depend on the ion implanted dose. Therefore, the prediction of the critical amorphizing dose as a function of the implant parameters is of great relevance for technological purposes, as it significantly affects dopant diffusion and activation.

Under traditional models, amorphization is envisaged to occur through the overlap of isolated damaged regions created by individual ions (heterogeneous amorphization) or via the buildup of simple defects (homogeneous amorphization). The heterogeneous mechanism is typical of heavy ions in Si and prevalent at low temperature, while the second occurs for light ions and high temperature regime. The morphology of the damage accumulation is completely different in the two cases, damage and amorphous pockets are typically observed in the heterogeneous amorphization. For cluster ion implantation, the mechanism of damage generation can be totally different from the corresponding monoatomic case since it is related to the simultaneous deposition of energy carried by cluster atoms,[5] resulting practically impossible to predict the amorphization conditions for specific cases. The morphology of the damage accumulation has never been experimentally investigated as a function of the atomic implanted dose in samples implanted with cluster ion beam.

In this article the amorphization process associated with cluster implants has been studied by cross-sectional transmission electron microscopy (TEM) for phosphorus cluster (P_4) implants as a function of dose and directly compared to monomer ion implantation at same energy and doses.

II. EXPERIMENT

Si(100) wafers were implanted with P_4^+ cluster ions from SemEquip ClusterIon® source at room temperature at the energy of 5 keV/P atom and at nine different doses ranging from $1\times10^{13}/\mathrm{cm}^2$ to $1\times10^{15}/\mathrm{cm}^2$. P_4^+ ion beam current was 50 μA/ion (this means a factor 4 to have the equivalent current per atom, i.e., 200 μA/P atom). In order to compare the amorphous formation induced by monomer ion implants, monomer P^+ ions were implanted at the same relative energies, similar doses, and beam current of the cluster beam. A JEOL 2010F high-resolution transmission electron microscope (HRTEM) with on-axis multibeam imaging conditions was used to study cross sections of the implanted samples. Samples were prepared using a Dual-Beam FEI Strata DB 235 focused ion beam system.

TEM analysis was used to observe the formation of amorphous zones in a crystal lattice. The presence of the amorphous phase was confirmed using both selected area diffraction and fast Fourier transform analysis of high-resolution images.

[a]Author to whom correspondence should be addressed; electronic mail: lroma@ufl.edu

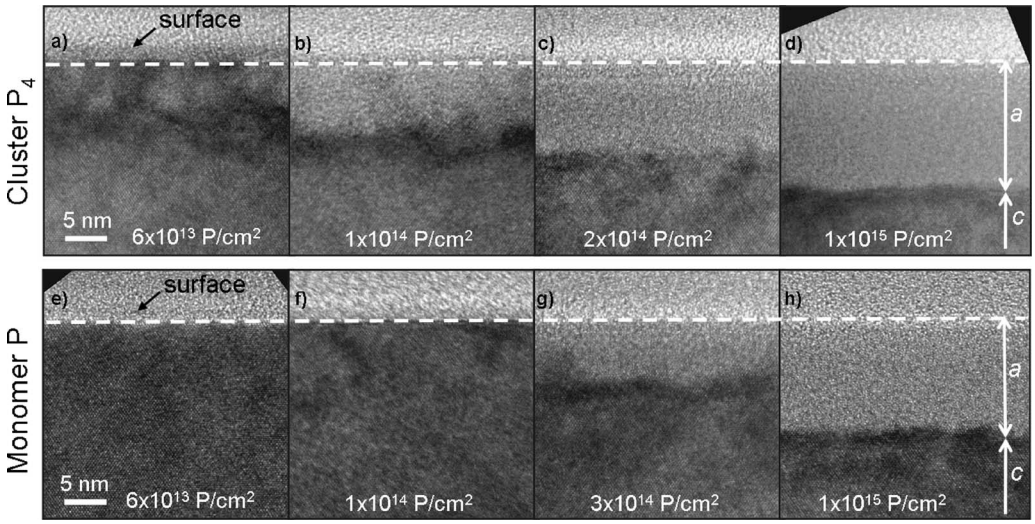

FIG. 1. Cross-sectional TEM images of samples implanted with 5 keV P_4^+ cluster [(a)–(d)] and P^+ monomer [(e)–(h)] beams at several doses. Cluster implants: (a) clearly amorphous pockets; (b) amorphous layer with crystalline pockets; [(c) and (d)] continuous amorphous layer (see Table I for further details). Monomer implants: [(e) and (f)] defects; amorphous layer with crystalline pockets; and (h) continuous amorphous layer. Amorphous (*a*) and crystalline (*c*) phases have been indicated in (d) and (g).

III. RESULTS AND DISCUSSION

Figure 1 shows cross-sectional HRTEM images of P_4^+ cluster (top) and monomer P^+ (bottom) implanted samples at several doses. Morphological details observed in cross-sectional TEM images are reported in Table I. In cluster implanted samples at doses between 1×10^{13} and 4×10^{13} cm^{-2} (not shown here), only damage pockets are visible and the damage depth is about 9 nm, while at 6×10^{13} cm^{-2} [Fig. 1(a)] clearly amorphous pockets appear. This suggests that damage morphology is governed by local melting in the cascade core which upon resolidification results in local amorphous pockets, typical of heterogeneous amorphization.[4] The amorphous layer develops from isolated pockets to a semi-continuous amorphous layer (at 1×10^{14} cm^{-2}) and finally to a continuous amorphous layer 7 nm thick after a dose of 2×10^{14} cm^{-2} [Fig. 1(c)]. Increasing the dose past that point continues to make the amorphous layer deeper and the amorphous/crystalline interface becomes smoother [Fig. 1(d)]. When a continuous amorphous layer is settled, the interface roughness decreases from 3 nm (at 2×10^{14} cm^{-2}) to 1 nm (at 1×10^{15} cm^{-2}). Monomer P^+ implanted samples at similar doses of cluster implants show that amorphization is less effective and amorphous regions begin to appear at doses of 3×10^{14} cm^{-2} [Fig. 1(g)], indicating that a higher dose is necessary to form a continuous amorphous layer. These data confirm the amorphization threshold for P implanted Si is around 5×10^{14} cm^{-2} at room temperature.[6]

The measured amorphous depths for P_4 (reported in Table I) and P implants have been plotted as a function of the P implanted dose in Fig. 2. The onset of continuous amorphous layer is indicated for both cluster (solid arrow) and monomer (dotted arrow) implants. The amorphous thickness before the formation of the continuous layer (at dose lower than 2×10^{14} cm^{-2}) has been measured as the minimum size of the amorphous pockets and it is indicative of the progressive increasing of amorphous regions to cost of the crystalline

TABLE I. TEM results for 5 keV P_4 cluster beam implanted samples. Minimum and maximum values are reported when a single depth is not characterizing.

Dose (at/cm^2)	Damage depth (nm)	Amorphous depth (nm)	Structure details	Amorphous/crystalline interface roughness (nm)
1.0×10^{13}	8.6–9.7		Damage pockets	
2.0×10^{13}	8.6–9.4		Damage pockets	
4.0×10^{13}	8.3–9.4		Damage pockets	
6.0×10^{13}	8.6–10.3	2.9–4.3	Clearly amorphous pockets	
8.0×10^{13}	10.3	7.1–7.7	Both amorphous and crystalline phases at same ratio	
1.0×10^{14}	11.4	7.1–8.3	Amorphous with crystalline pockets	
2.0×10^{14}	14.3	8.6–10.0	Continuous amorphous layer	~3.0
5.0×10^{14}	15.1	11.4–12.9	Continuous amorphous layer	~1.5
1.0×10^{15}	16.3	13.4–14.3	Continuous amorphous layer	~1.0

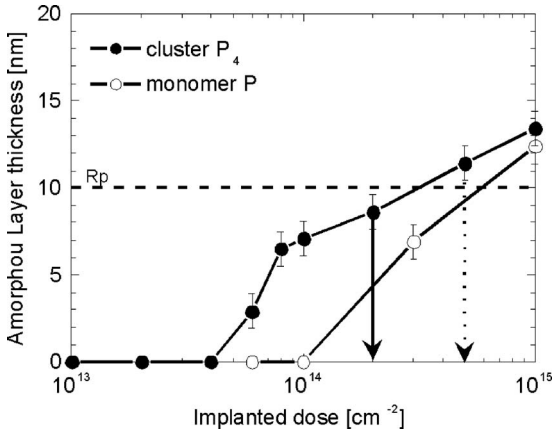

FIG. 2. Amorphous layer thickness measured by TEM in 5 keV P_4^+ cluster (full symbols) and monomer (empty symbols) implanted samples vs implanted dose. The solid line arrow indicates the formation of continuous amorphous layer by cluster ion implantation measured in this work. Amorphization threshold by monomer ion implantation (dotted line arrow) is also indicated. 5 keV P projected ranges is indicated.

material. The depth of the amorphous layer at the threshold dose is about the 5 keV P^+ ions projected range ($R_p \sim 10.0$ nm calculated by SRIM-2007 simulation code[7]). This condition is critical for the dopant activation in self-amorphizing impurity implant since it allows activating the maximum dopant concentration. The reliability of this condition strongly depends on ion species and energy, and it is not always accessible with monomer implants. Instead, one can simply modify the cluster size in order to realize this condition for each ion species, once the amorphization threshold is known.

For P_4^+ implant, the cluster amorphizing threshold dose is at least 2.5 times lower than the dose required by P monomer implant. A similar reduction (2.8) has been observed also for As_4 clusters (not shown), B_xH_y and C_x clusters have been reported to produce thicker amorphous layer than the relative monomer implants.[8,9] Since the same average beam current was used in both monomer and cluster P implants, an instantaneous dose rate effect[10] due to the simultaneous impact of four P atoms per cluster can be claimed as responsible for the amorphization threshold reduction. The simultaneous deposition of energy carried by the four atoms in a cluster on the surface region close to the impact point creates overlapping cascades, which are more effective to damage the crystal than four consecutively impinging ions. Gibbon's model[11] of heterogeneous amorphization predicts the damage rate when overlap of ion collision cascades is necessary to convert the crystalline material into amorphous; a superlinear damage growth is expected with increasing the number of overlap, this case has been observed for amorphization induced by light ions irradiation at room temperature. The same model can be extended to understand the general behavior of the cluster-size dependence of the ion implantation damage. The nonlinear effect with increasing the cluster size is caused by overlapping of temporary damage areas created by the constituent atoms in the cluster. Shao and co-workers[12–14] observed this superlinear damage by measuring the fraction of displaced Si atoms by Rutherford backscattering spectrometry (RBS) in samples implanted with C, Cu, and Au clusters: the superlinear effect looks to be particularly enhanced at low cluster size, in contrast with the molecular dynamics prediction by Aoki *et al.*[15] Our TEM analyses showed that not only the small clusters produce much more damage than the corresponding monomer implant but also the morphology of the damage is different. The formation of amorphous pockets at dose of 6×10^{13} cm^{-2} in the cluster implanted sample is indicative of a denser collision cascade, while no pockets are visible in the monomer case at the same and even also at higher doses. This observation is important to develop further modeling of the amorphization mechanism. In fact, according to Gibbon,[11] the amorphization threshold dose depends inversely on the effective damaged volume in the ion collision cascade. Therefore, the effective damaged volume associated with each cluster (V_{cd}) results to be bigger than that of the single monomer ions (V_{md}). If the monomer implant amorphizes through a direct cascade mechanism, the damage growth rate is simply done by the following formula:[11]

$$f = 1 - \exp\left(-\frac{V_{md}}{\Delta r}\phi\right), \tag{1}$$

where f is the amorphized fraction, Δr is the mean projected range, and ϕ is the ion implanted dose. In this simple case, the ratio between the amorophizing doses for cluster and monomer implants will be

$$\frac{\phi_m}{\phi_c} = \frac{V_{cd}}{n}\frac{1}{V_{md}}. \tag{2}$$

Since V_{cd} is created by the overlapping cascades of the single atoms in the clusters, it will strongly depends on the cluster size, on the number of overlap, and on the atomic species. In our experiment we found $\phi_m/\phi_c = 2.5$ and therefore $V_{cd}/4 = 2.5V_{md}$, so the effective damaged volume per P atom is 2.5 times higher in the case of clusters with respect to the corresponding monomer beam implant. RBS data from Wang *et al.*[14] indicate similar findings: $\phi_m/\phi_c \sim 1.34$ and 3.7 for Cu_2 and Cu_6 clusters, respectively.

IV. CONCLUSIONS

In conclusions, the morphology of the amorphization process by cluster P_4 and P monomer ion beam has been investigated for the first time by cross-sectional HRTEM analyses, revealing substantial differences between the two cases. The amorphization threshold dose for P_4 cluster implant is 2×10^{14} cm^{-2}, which is lower than the dose required for the relative monomer ion induced amorphization by a factor of 2.5. This phenomenon, typical of cluster beam implantation, is due to the simultaneous deposition of energy by the atoms that constitute the cluster.

ACKNOWLEDGMENTS

The authors would also like to thank the Major Analytical and Instrumentation Center at the University of Florida for access to their characterization tools.

[1]W. A. Krull, B. Haslam, T. Horsky, K. Venheyden, and K. Funk, AIP Conf. Proc. **866**, 182 (2006).
[2]E. Landi, A. Armigliato, S. Solmi, R. Köghler, and E. Wieser, Appl. Phys. A: Mater. Sci. Process. **47**, 359 (1988).
[3]S. Solmi, E. Landi, and F. Baruffaldi, J. Appl. Phys. **68**, 3250 (1990).
[4]L. Pelaz, L. A. Marqués, and J. Barbolla, J. Appl. Phys. **96**, 5947 (2004), and references therein.
[5]L. A. Marqués, L. Pelaz, I. Santos, and V. C. Venezia, Phys. Rev. B **74**, 201201 (2006).
[6]F. F. Morehead, B. L. Crowder, and R. S. Title, J. Appl. Phys. **43**, 1112 (1972).
[7]J. F. Ziegler, J. P. Biersack, and U. Littmark, *The Stopping and Range of Ions in Solids* (Pergamon, New York, 1985).
[8]S. Heo, H. Hwang, H. T. Cho, and W. A. Krull, Appl. Phys. Lett. **89**, 243516 (2006).
[9]W. Krull, B. Haslam, T. Horsky, K. Verheyden, and K. Funk, AIP Conf. Proc. **866**, 182 (2006).
[10]P. J. Schultz, C. Jagadish, M. C. Ridgway, R. G. Elliman, and J. S. Williams, Phys. Rev. B **44**, 9118 (1991).
[11]J. F. Gibbons, Proc. IEEE **60**, 1062 (1972).
[12]L. Shao, M. Nastasi, X. Wang, J. Liu, and W. Chu, Nucl. Instrum. Methods Phys. Res. B **242**, 503 (2006).
[13]Z. X. Xie, X. M. Wang, X. M. Lu, L. Shao, J. R. Liu, and W. K. Chu, AIP Conf. Proc. **576**, 987 (2001).
[14]X. M. Wang, H. Chen, L. Shao, J. R. Liu, and W. K. Chu, Nucl. Instrum. Methods Phys. Res. B **196**, 100 (2002).
[15]T. Aoki, T. Seki, J. Matsuo, Z. Insepov, and I. Yamada, Nucl. Instrum. Methods Phys. Res. B **153**, 264 (1999).